Atmos. Chem. Phys. Discuss., 15, 15683–15710, 2015
www.atmos-chem-phys-discuss.net/15/15683/2015/
doi:10.5194/acpd-15-15683-2015

Atmospheric Chemistry and Physics Discussions
Open Access

The regional distribution characteristics of aerosol optical depth over the Tibetan Plateau

C. Xu[1,2,3,*], Y. M. Ma[1,3,*], C. You[1,2], and Z. K. Zhu[1,2,3,4]

[1]Key Laboratory of Tibetan Environment Changes and Land Surface Processes, Institute of Tibetan Plateau Research, CAS Center for Excellence in Tibetan Plateau Earth Sciences, Chinese Academy of Sciences, Beijing 100101, China
[2]University of Chinese Academy of Sciences, Beijing 100049, China
[3]Qomolangma Station for Atmospheric Environmental Observation and Research, Chinese Academy of Sciences, Dingri 858200, Tibet, China
[4]Cold and Arid Regions Environmental and Engineering Research Institute, Chinese Academy of Sciences, Lanzhou 730000, China
[*]now at: Institute of Tibetan Plateau Research, CAS Center for Excellence in Tibetan Plateau Earth Sciences, Chinese Academy of Sciences, Beijing, China

Received: 4 May 2015 – Accepted: 21 May 2015 – Published: 11 June 2015

Correspondence to: Y. M. Ma (ymma@itpcas.ac.cn) and C. Xu (xuchao@itpcas.ac.cn)

Published by Copernicus Publications on behalf of the European Geosciences Union.

Abstract

The Tibetan Plateau (TP) is representative of typical clean atmospheric conditions. Aerosol optical depth (AOD) retrieved by Multi-angle Imaging SpectroRadiometer (MISR) is higher over Qaidam Basin than the rest of the TP all the year. Different monthly variation patterns of AOD are observed over the southern and northern TP, whereby the aerosol load is usually higher in the northern TP than in the southern part. The aerosol load over the northern part increases from April to June, peaking in May. The maximum concentration of aerosols over the southern TP occurs in July. Aerosols appear to be more easily transported over the main body of the TP across the northeastern edge rather than the southern edge. This is may be because the altitude is much lower at the northeastern edge than that of the Himalayas located along the southern edge of the TP. Three-dimensional distributions of dust, polluted dust, polluted continental and smoke are also investigated based on Cloud-Aerosol Lidar and Infrared Pathfinder Satellite Observation (CALIPSO) data. Dust is found to be the most prominent aerosol type on the TP, and other types of aerosols affect the atmospheric environment slightly. A natural boundary seems to extend to an altitude of 6–8 km a.s.l., which may act as a dividing line of higher dust occurrence in the northern TP and lower dust occurrence in the southern TP, especially in spring and summer. This boundary appears around 33–35° N in the middle of the plateau, and it is possibly associated with the high altitude terrain in the same geographic location. Comparisons of CALIPSO and MISR data show that this natural boundary extending to upper troposphere is consistent with the spatial pattern of aerosol loading. The whole TP blocks the atmospheric aerosols transported from surrounding regions, and the extreme high mountains on the TP also cause an obstruction to the transport of aerosols. The aerosol distribution patterns are primarily driven by atmospheric circulation. Northerly winds prevail above the TP in spring, which also facilitates the transport of aerosols from the Tarim Basin and Qaidam Basin to the main body of the TP. Nevertheless, aerosols above the TP can originate from both the northern and southern sides of the TP during summer.

ACPD
15, 15683–15710, 2015

1 Introduction

The Tibetan Plateau (TP), located in central eastern Eurasia, is the most prominent and complex terrain feature on the Earth. It has the world's highest average elevation (about 4000 m), with some surface features even reaching into the mid-troposphere. Due to its topographic characteristics, the TP surface absorbs high quantities of solar radiation with corresponding impacts on surface heat or water fluxes (Ma et al., 2014a, b). The East Asian monsoon and the eastern part of the South Asian monsoon systems are mainly controlled by the thermal forcing of the TP (Wu et al., 2007, 2012).

Many studies have focused on environmental and climate change over the TP (Xu et al., 2009; Ma et al., 2011; Lin et al., 2012; Yao et al., 2012; Sheng et al., 2013), and the TP environment is greatly affected by natural and anthropogenic aerosols from the surrounding regions (Z. Liu et al., 2008; Bucci et al., 2014; Cong et al., 2015). Therefore, studying tropospheric aerosols and their effects on the TP is of great importance (King et al., 1999; Kaufman et al., 2002; Li et al., 2011). Vernier et al. (2011) reported the presence of an aerosol layer at the tropopause level above Asia during the monsoon season. The Taklimakan and Gobi deserts are two major dust sources with long-range transport mainly occurring in spring (D. Liu et al., 2008). Summertime Tibetan airborne dust plumes were detected from the Cloud-Aerosol Lidar and Infrared Pathfinder Satellite Observations (CALIPSO) satellite (Huang et al., 2007), and Xia et al. (2008) suggested that the aerosol load in summer over the TP was mainly associated with the Taklimakan desert. Dust above the TP appears to be largely related to source regions to the north and on the eastern part of the TP (Z. Liu et al., 2008). The impact of aerosols above and around the TP during pre-monsoon season was also investigated, however, a strong elevated heating which could influence large-scale monsoonal circulations was not found (Kuhlmann and Quaas, 2010). Anthropogenic emissions from strong pollution events can occasionally be transported to the central TP by prevailing southwesterly winds (Xia et al., 2011). The high altitudes of the Himalayas appear to block most BC particles intruding into the TP, but the Yarlung Tsangpo River valley serves as a "leak" by which contaminants can reach the southeast TP (Cao et al., 2010). The southern and northern TP are under the control of different climate systems (Tian et al., 2007; Yao et al., 2013). Some previous studies indicated that the southern and northern TP possibly presented different variations in aerosol properties, e.g. different temporal variations in dust storm records (Wu et al., 2013). However, the mechanisms of those differences still need further study.

Although the aerosol load is relatively low, aerosols over the TP have the unique characteristics. In this study, the seasonal variations and spatial distributions of aerosols over the TP are presented based on the Multi-angle Imaging SpectroRadiometer (MISR) data. The seasonal vertical distributions of dust, polluted dust, polluted continental and smoke aerosols are also investigated using the CALIPSO data. This study might indicate a natural boundary between the northern and southern TP exist in the middle of the plateau. Besides that, the spatial patterns of aerosol loading are consistent with the vertical distributions of aerosols. We preliminarily propose the possible mechanisms for the aerosol distributions.

2 Data and methodology

The MISR was successfully launched into sun-synchronous polar orbit aboard Terra, NASA's first Earth Observing System (EOS) spacecraft, on 18 December 1999. Viewing the sunlit Earth simultaneously at nine widely-spaced angles, MISR provides radiometrically and geometrically calibrated images in four spectral bands at each of the angles. The spatial resolution of the operational MISR aerosol retrieval algorithm is 17.6 km × 17.6 km. The retrieval region has 16 × 16 subregions, and each subregion covers a 1.1 km × 1.1 km area. MISR aerosol retrievals have been evaluated by many studies (Martonchik et al., 2004; Kahn, 2005; Kahn et al., 2010; Witek et al., 2013). The accuracy of MISR AOD was much better than MODIS AOD over the TP (Abdou et al., 2005; Xia et al., 2008). In this study, daily Level 3 MISR aerosol data from March 2000

ACPD
15, 15683–15710, 2015

to December 2014 are used to investigate the aerosol spatial distribution, and the spatial resolution of MISR data is 0.5° × 0.5°.

Monthly variations of AOD at 558 nm are analyzed over the TP. If there was only one satellite observation for a month then this grid value in that particular month was excluded for that year, since there would be too few observations to represent the monthly average. The monthly means that represent the aerosol long-term distribution are calculated by averaging the observation data for that month in each year. To analyze aerosol zonal average, only aerosol retrievals over the TP (27–40° N, 75–105° E) at elevations higher than 3000 m are used. In this study, the northern part of the TP is defined as the region north of 33–34° N, and the southern part of the TP is defined as the region south of 33–34° N. The reason for selecting 33–34° N is based on the distributions of aerosols, which appear to show different patterns to the north and south of this latitude.

The Cloud-Aerosol Lidar and Infrared Pathfinder Satellite Observation (CALIPSO) satellite provides new insight into clouds and atmospheric aerosols (Winker et al., 2007, 2010). The CALIPSO satellite was launched into a Sunsynchronous orbit on 28 April 2006, with a 16 day repeating cycle. The lidar level 3 aerosol product is a quality screened aggregation of level 2 aerosol profile data. A series of filers are designed to eliminate samples and layers that were detected or classified with very low confidence or that have untrustworthy extinction retrievals (Winker et al., 2013). The CALIPSO version 1.00 and version 1.30 level 3 aerosol profile data from March 2007 to February 2015 are used in this study. Nighttime all-sky data are used, because the instrument is more sensitive during nighttime than daytime without solar background illumination (Winker et al., 2013). The spatial resolution of level 3 data is 5° × 2° (longitude–latitude), and the vertical resolution is 60 m observed from −0.5 to 12 km a.s.l. (a.s.l., the altitude below is a.s.l. without a specific instruction) in the troposphere. The primary variable of aerosol type is used, and this variable counts the number of aerosol samples having each aerosol type for each latitude/longitude/altitude grid cell. Six aerosol types including clean marine, dust, polluted continental, clean continental, polluted dust, and smoke are classified. From the data product descriptions, the composition of six aerosol types can be known. Clean marine is a hygroscopic aerosol that consists primarily of sea-salt (NaCl). Dust is mostly mineral soil. Polluted continental is background aerosol with a substantial fraction of urban pollution. Clean continental is a lightly loaded aerosol consisting of sulfates (SO_4^{2-}), nitrates (NO_3^-), organic carbon (OC) or Ammonium (NH_4^+). Polluted dust is a mixture of desert dust and smoke or urban pollution. Smoke aerosol consists primarily of soot and OC. Mixtures of two aerosol types are not assigned to one aerosol sample. Dust, polluted dust, polluted continental and smoke possibly influence the TP (Kuhlmann and Quaas, 2010). The aerosol samples for these major types in each season were calculated by accumulating the detected samples for the season in each latitude/longitude/altitude grid cell. The multi-year aerosol samples for each season are obtained by averaging across multiple years. There are uncertainties associated with incorrect aerosol type classification, and these uncertainties further affect aerosol extinction. Aerosol extinction coefficients are not analyzed due to too low values with high uncertainties over the TP. In this study, four common seasons are defined, respectively, as March to May (spring), June to August (summer), September to November (autumn) and December to February in the next year (winter).

The meridional circulations are examined using ERA-interim monthly mean reanalysis data, produced by the European Centre for Medium-Range Weather Forecasts (ECMWF). The spatial resolution of ERA-interim reanalysis data is $0.75^{\circ} \times 0.75^{\circ}$, and data are analyzed from March 2000 to February 2014.

3 Results and analysis

3.1 Aerosol distribution characteristics

Monthly variations of AOD over the Tibetan Plateau are shown in Fig. 1. Seasonal variations of AOD are significant. The monthly average of AOD for the ~ 10 years study

ACPD
15, 15683–15710, 2015

period was less than ∼ 0.50 over the whole TP in spring and summer, but less than 0.25 in autumn and winter. The aerosol load increases gradually from March to May over the northern part of the TP, while it decreases from June to August. The areas with higher aerosol loads (> 0.25) expand gradually in April and reach their maximum extent in May, which indicates AOD is highest in May. AOD is also higher during April to June (> 0.50) than in the other months over Tarim Basin. AOD is higher to the north of 33–34° N than to the south all the year. The east–west trending mountains on the TP seem to act as a major natural barrier for the transport of atmospheric aerosols from north to south. The aerosol load increases slightly to the south of 30° N in summer. The aerosol load over the southern TP may be associated with the Indo-Gangetic Plains. A possible explanation of this phenomenon may be the peaks in anthropogenic emissions in the Indo-Gangetic Plains during summer coupled with suitable atmospheric circulation. Alpine valleys along the Himalayas (e.g. the Pulan valley in the western Himalayas and the Yadong valley in the middle Himalayas) may act as channels along which aerosols can be transported into the southern part of the TP during the monsoon season. In autumn and winter, AOD over the whole TP is mostly lower than 0.20, except in the Qaidam Basin. AOD even decreases below 0.10 over most regions of the TP from November to January. Unfortunately, AOD over the southeast TP cannot always be determined in each season due to thick cloud or high precipitation.

In summary, AOD is usually higher over the Qaidam Basin than over the other parts of the TP, throughout the year. The aerosol loads are generally higher over the northern TP than over the southern part, especially during April to June. The northeastern edge of the TP, especially the Qaidam Basin, may provide transport channels along which dust or anthropogenic emissions can be transported onto the TP. The aerosol load reaches extremely high values over the Tarim Basin and northern India in each month. Seasonal variations of AOD show much higher values in spring and summer than values in autumn and winter.

3.2 Zonal variations in aerosol properties over the TP

Although the aerosol load is quite low over the TP, the zonal distribution pattern can be seen clearly. Figure 2 shows the zonal monthly means of AOD for a period of over ten years. AOD is usually higher in the northern part than in the southern part. Monthly variations in the northern TP are different from those in the southern TP. The aerosol load in the northern TP is relatively high from March to August, but especially during April to June. Correspondingly, AOD in the southern part increases from June to August. The maximum monthly mean of AOD in the northern TP occurs in May, while the maximum monthly mean in the southern part occurs in July. This is in accordance with previous surface observations (Gobbi et al., 2010; Xu et al., 2014). The monthly zonal averages of AOD are higher than 0.22 over the northern part during April to June, while they are lower than 0.26 over the southern part. The monthly zonal peak in the northern TP is about 1.5 times that in the southern part. The zonal means over the whole TP are below 0.10 during November to January.

Overall, AOD shows clear zonal distributions. Different monthly variation pattern of AOD is shown in the northern part and southern part of TP. The maximum aerosol concentration is observed during April to June to the region north of 33–34° N, with maximum levels in May. Aerosols can be clearly transported to the south of about 30° N over the TP, with maximum levels in July.

3.3 Vertical distributions of aerosols

Dust, polluted dust, polluted continental and smoke retrieved by CALIPSO are the major aerosol types, possibly influencing the environment over the TP. The seasonal vertical distributions of these aerosol types are discussed along the latitudinal transects. The regions from 80 to 100° E covering most of the TP are selected to represent aerosol three-dimensional distributions.

Figure 3 shows latitudinal transects of accumulated dust samples in each season. The features of aerosol three-dimensional distributions can be concluded to seasonal

ACPD
15, 15683–15710, 2015

variability and spatial differences. Dust generation and lofting is always active over the Tarim Basin and Hexi Corridor during the four seasons, while dust occurs frequently over the northern Indian peninsula only in spring. Detected dust over the TP increases significantly in spring and summer, and dust occurs much less frequently in autumn and winter. This phenomenon possibly indicates that dust can be transported into the TP in spring and summer, while dust only occurs in Qaidam Basin in autumn and winter. Much less dust is detected on-plateau than off-plateau, which indicates that the TP acts as a large barrier for the transport of dust. Furthermore, dust occurrence decreases from the surface to the high altitude. Most of Tibetan airborne dust is concentrated at a height of less than 7 km during spring and summer. Obvious differences of detected dust exist between the southern and northern TP in spring and summer. Dust occurs more frequently over the northern part of TP than the southern part. The boundary between high dust occurrence over the northern TP and relatively low dust occurrence over the southern TP is clear along each longitudinal cross section. The boundary runs east to west across the TP, which appears to be in accord with the distributions of monthly MISR AOD. After climbing the northern edge of the TP, dust reduces substantially. The extreme high mountains over the TP include the Kunlun, the Tangula and the Gangdise. When dust encounters these major mountains one by one, the detected dust aerosols passing through the mountains decrease gradually along the longitudinal zones from north to south in each season. The dust layer has the greatest depth over all the longitudinal zones in spring, followed by summer. In spring, dust forming the layer extends from the surface to 10–11 km over the TP. Dust can be generated and lofted to a similar altitude over the Tarim Basin and Hexi Corridor in spring, whereas dust layer exhibits a lesser thickness and extends to 6–8 km over the northern Indian peninsula. The boundary of dust occurrence between the northern and southern TP can be seen clearly from surface to a height of about 6–8 km, while it becomes unapparent at high altitudes. Dust layer can only extends to the altitudes of 8–10 km over the TP during summer, and the boundary appears to be obvious at an altitude of less than 7 km. Dust occurs much less frequently above the TP in autumn

ACPD
15, 15683–15710, 2015

and winter, and some dust can be only detected to the north of about 35° N in 90–95 and 95–100° E transects – the Qaidam Basin. Dust layer is usually at altitudes of less than 8 km in autumn and winter. This phenomenon may indicate that dust seems to be transported more easily through the northern edge of TP than the southern edge, especially in spring and summer. Due to low dust occurrence, the differences of detected dust between the northern and southern TP are not obvious in autumn and winter.

Figure 4 shows latitudinal transects of accumulated polluted dust samples in each season. Polluted dust also affects the environment of the TP. Nevertheless, the effect of polluted dust is not as significant as dust. High occurrence of polluted dust is observed over the northern Indian peninsula, except in summer possibly due to large precipitation. The occurrence of polluted dust is higher than dust over the northern Indian peninsula except in spring. The polluted dust is confined to the lower 5 km of the atmosphere over the northern Indian peninsula in spring, while polluted dust is concentrated at a height of less than 4 km in other seasons. The maximum height seems to be crucial to the long-range transport of polluted dust, considering that it is comparable to or lower than the altitude of the TP. Polluted dust cannot be transported onto the TP, when its maximum height is lower than the southern edge. Polluted dust also occurs to the north of the TP, but the effect is not obvious. Polluted dust decrease dramatically on-plateau relative to off-plateau regions. Only a small amount of polluted dust can be detected over the TP, and the number of polluted dust samples is a bit larger in spring and summer than in autumn and winter. The polluted dust layer also exhibits a relatively greater thickness in spring and summer. From the surface to the top layer, there are no significant changes in the occurrence of polluted dust in each season. Differences of occurrence between the northern and southern part of TP also seem to be unapparent. Polluted dust rarely occur in autumn and winter, especially along the longitudinal cross section of 80–85, 85–90 and 90–95° E. It is worthy of thinking about the sources of polluted dust above the TP.

Figure 5 shows latitudinal transects of accumulated polluted continental samples in each season. Much less polluted continental samples are detected relative to dust

ACPD
15, 15683–15710, 2015

or polluted dust over the study regions. This result does not mean that there is less urban air pollution in essence. Urban pollution mixed with dust is classified as polluted dust. Possible explanation of this result is that urban pollution mixed with dust happens more frequently rather than only urban pollutant. Polluted continental aerosols seem to happen more frequently in autumn and winter over the northern Indian peninsula. Polluted continental aerosols hardly have any impact on the TP in each season.

Figure 6 shows latitudinal transects of accumulated smoke samples in each season. Smoke consisting of soot and OC can be transported to the main body of the TP. Smoke occurrence is higher over the southern side of the TP than the northern side. In spring, few smoke samples are detected above the TP, and do not show a continuous vertical distribution. This indicates smoke released during big fires can be occasionally uplifted above the atmospheric boundary layer and further transported to the TP. Detected smoke samples increase lightly over the TP during summer, and they are also not continuous in column. Although smoke does not occur during summer as frequently as autumn or winter over the northern Indian peninsula, strong southerly winds blow towards the TP only during summer. Smoke can even suspend at an altitude of 12 km over the TP in summer. Detected smoke samples decrease again in autumn, and smoke usually occurs less than 7 km. Smoke occurrence is a bit higher in the southern part of the TP than the northern part in summer and autumn. Smoke appears to be more likely transported from the northern Indian peninsula to the TP in summer and autumn, because higher occurrence of smoke is shown in the adjacent regions of the southern edge. No smoke samples are detected over the TP in winter.

In summary, pure dust is found to be the main aerosol type above the TP, and dust mixed with pollutions or smoke occasionally occurs. Smoke only has a little effect on the TP in summer, while urban pollutions do not contaminate the environment of the TP individually. Much less aerosols are detected on-plateau than off-plateau, which indicates the TP acts as a natural barrier. Dust and polluted dust exhibit more thickness in spring and summer above the TP. The bulk of dust is concentrated at a height of less than 7 km during spring and summer. A boundary of dust occurrences between the northern and southern TP can be found clearly in spring and summer, and this boundary extending to an altitude of 6–8 km appears to be apparent. The occurrences of polluted dust, smoke or polluted continental aerosols do not show any boundary over the TP. Smoke aerosols may be more likely to come from the northern Indian peninsula in summer.

3.4 Possible factors contributing to the aerosol distribution pattern

The TP has quite pristine atmospheric conditions, that is to say, aerosols hardly come from local contributions. There are no obvious source regions of biomass burning or urban pollutants on the TP. As the most prominent aerosol type on the TP, airborne dust on the TP mostly comes from the surrounding regions. Negative or significant negative relationship between AOD and wind speed was found over most regions of the TP based on the previous results (Ge et al., 2014). Therefore, long-range transport of aerosols primarily impacts the atmospheric environment over the TP, and the contribution of inner sources on the TP is ignored in our analysis. The aerosol load has significant seasonal variations. Interestingly, the pattern of seasonal variations over the northern TP is different to that of the southern part: this could be due to many factors, including high altitude terrain and atmospheric circulation.

The high terrain acts as a natural barrier for the transport of atmospheric aerosols from the surrounding polluted regions to the main body of the TP due to its topographic characteristics. Therefore, AOD over the TP is much lower than that of surrounding regions, such as the Taklimakan desert and Indo-Gangetic Plains. Moreover, the altitude is lower on the northeastern TP relative to that of the other parts, while altitude along the southern edge is quite high (Fig. 7). When aerosols pass across the northeastern edge, the major natural obstacles they encounter are several mountains. The Kunlun and the Tangula mountains that appear from northwest to southeast act as the barriers to block aerosols. It is then difficult for aerosols to spread further southward. The aerosol load shows higher values over the northern part than over the southern part. This phenomenon may be related to the terrain of the TP. The high aerosol load occur-

ACPD
15, 15683–15710, 2015

Regional distribution characteristics of aerosol optical depth

C. Xu et al.

ring over the northern part seems to be associated with lower altitudes, and a relatively low aerosol load along the southern edge seems to be associated with the higher altitudes. Aerosols are more easily transported onto the TP through the northeastern edge rather than across the southern edge. This is may be because the altitude is much lower at the northeastern edge than that of the Himalayas located along the southern edge of the TP. Aerosols may only pass through alpine valleys along the Himalayas to intrude into the TP, while a broader northeastern edge – especially the Qaidam Basin – seems to provide transmission channels. Aerosols are rarely transported onto the TP across other parts of the Himalayas Mountains. The Gangdise and the Nyainqen-tanglha mountains are located around 30–31° N on the southern TP. Even if a small quantity of aerosols climb and pass through the Himalayas, it is also difficult for the pollutants to spread further northward to the main body of the TP. Similar phenomenon is also observed in the vertical distributions of dust aerosols. The dust occurrence is much higher in the northern TP than the southern TP during spring and summer. The boundary even extends from the surface to the altitude of 6–8 km, which can be seen clearly. This boundary acts as a dividing line of higher dust occurrence in the northern TP and lower dust occurrence in the southern TP. Besides that, the boundary extending to a height seems to exist only in dust aerosols, while it is not apparent in other types of aerosols due to their small amounts. The high altitude terrain located around 33–35° N in the middle of the plateau appears to be geographically identical to this natural boundary. The whole TP blocks the atmospheric aerosols, and the extreme high mountains on the TP also cause an obstruction to the transport of aerosols.

Atmospheric circulation also greatly impacts the seasonal aerosol variations. Figure 8 shows the annual average vertical wind fields. A longitude of 95° E, corresponding to the Qaidam Basin, is chosen to analyze the vertical atmospheric circulations. In spring, air flows indicate updrafts below 300 hPa to the north of the TP, and downdrafts to the south of the TP. Northerly winds prevail over the whole TP. The atmospheric circulation promotes the transport of aerosols from the Tarim Basin and Qaidam Basin to the main body of the TP. In other words, aerosols above the TP are mostly from

ACPD
15, 15683–15710, 2015

the northern side of the TP in spring. Aerosols transported to the southern TP reduce substantially after passing through the northern TP. The atmospheric circulation primarily leads to higher aerosol loading in the northern TP and lower aerosol loading in the southern TP. Meanwhile the atmospheric circulation also affects the different vertical distributions of aerosol occurrences extending to upper troposphere. During summer, the airflows primarily originating from both the northern and southern sides of the TP carry aerosols to the main body of the TP. Airflows with two directions meet around 33–34° N in the middle of the TP. The intersection of airflows from northern and southern sides is nearly located at the same geographic location. It might be reasonably deduced that atmospheric circulation partly leads to the formation of this natural boundary in the middle of plateau. Meanwhile strong updrafts are clearly shown on both the northern and southern parts of the TP. This vertical circulation can facilitate the transport of atmospheric aerosols from the source regions, like the Indo-Gangetic Plains and Tarim Basin, to the main body of the TP. The strong southerly winds can provide the dynamical condition for the transport of aerosols during monsoon season, which leads to the highest aerosol load occurring in July on the southern TP. Dust particles coated by pollution acids can provide the predominant source of cloud condensation nuclei (Ma et al., 2010). Urban emissions consisting of hygroscopic compounds could be deposited by heavy precipitation and reduce substantially. As a result, the aerosol particles continue to reduce drastically after passing through the Himalayas mountains due to the physical blocking. Consequently, the aerosol loading and occurrences are still higher in the northern TP than the southern TP during summer. During autumn, weak updrafts can be observed on the northern and southern sides of the TP. In winter, the vertical circulation flows even have a negative impact on the transport of aerosols originating from the southern side of the TP. Seasonal variations of meridional circulations lead to the relatively higher aerosol loads in spring and summer on the TP.

ACPD
15, 15683–15710, 2015

4 Concluding remarks

This study identifies the patterns of aerosol variations over the TP using the 15 year MISR data. Furthermore, the vertical distributions of dust, polluted dust, polluted continental and smoke aerosols retrieved by 8 year CALIPSO data are also investigated over the TP. The possible reasons for the temporal variations and spatial distributions of aerosols are discussed.

Higher aerosol occurrences are observed on-plateau than off-plateau. Dust is found to be the major aerosol type above the TP, while polluted dust and smoke aerosols affect the atmospheric environment on the TP slightly. Polluted continental aerosols (urban pollutants) hardly affect the environment on the TP individually. Therefore, the aerosol load might be largely associated with dust occurrence. Higher aerosol loads are observed in spring and summer rather than in autumn and winter. Meanwhile, both the occurrence and the thickness of airborne dust also reach maximums in spring. Dust layer over the TP can be even detected at the altitudes of 11–12 km in spring, while it reduces obviously in other seasons. Most of airborne dust above the TP is concentrated in the lower 7 km of the atmosphere during spring and summer. AOD shows much higher values over Qaidam Basin than other parts of the TP throughout the year. Moreover, AOD is usually higher in the northern than the southern TP. Aerosols are found to be more easily transported onto the TP across the northeastern edge than across the southern edge. This distribution pattern of aerosol loading can be also reflected in the vertical distributions of aerosols. A natural boundary extending to an altitude of 6–8 km appears to be a dividing line of higher dust occurrence in the northern TP and lower dust occurrence in the southern TP during spring and summer. However, this boundary cannot be seen in the distributions of other aerosol types due to their low occurrences. The boundary around 33–35° N in the middle of the plateau might be associated with the high altitude terrain in the same geographic location. The high altitudes of topography on the TP can possibly block the transport of aerosols.

ACPD
15, 15683–15710, 2015

Besides that, the northern part and the southern part of the TP show distinct monthly variation patterns. The maximum monthly AOD over the northern TP occurs in May, and aerosols can even spread to the region north of 33–34° N. Aerosols transported to the south of ~ 30° N over the TP can be seen clearly, with maximum occurrence in July in the southern part. The monthly variations of aerosol load are greatly impacted by atmospheric circulation that directly controls where the air travels. Due to prevailing northerly winds, aerosols above the TP mainly originate from the northern side of the TP rather the southern side during spring. During summer, strong airflows from both the northern and southern sides blow towards the TP. Aerosol advection from both sides occurs, affecting the atmospheric environment on the TP. The atmospheric circulations also possibly contribute to the formation of different variation pattern on the southern and northern TP.

Acknowledgements. This research was funded by the Chinese Academy of Sciences (XDB03030201), the CMA Special Fund for Scientific Research in the Public Interest (GYHY201406001), the National Natural Science Foundation of China (91337212, 41275010) and EU-FP7 projects "CORE-CLIMAX" (313085). The MISR data were obtained from the NASA Langley Research Center Atmospheric Science Data Center. The CALIPSO data were obtained from the NASA Langley Research Center Atmospheric Science Data Center. The ERA-interim data were produced by ECMWF. The first author would like to acknowledge Changgui Lin and all the other group members for their help in preparing the paper.

References

Abdou, W. A., Diner, D. J., Martonchik, J. V., Bruegge, C. J., Kahn, R. A., Gaitley, B. J., Crean, K. A., Remer, L. A., and Holben, B.: Comparison of coincident Multiangle Imaging Spectroradiometer and Moderate Resolution Imaging Spectroradiometer aerosol optical depths over land and ocean scenes containing Aerosol Robotic Network sites, J. Geophys. Res.-Atmos., 110, D10S07, doi:10.1029/2004JD004693, 2005.

ACPD
15, 15683–15710, 2015

Bucci, S., Cagnazzo, C., Cairo, F., Di Liberto, L., and Fierli, F.: Aerosol variability and atmospheric transport in the Himalayan region from CALIOP 2007–2010 observations, Atmos. Chem. Phys., 14, 4369–4381, doi:10.5194/acp-14-4369-2014, 2014.
Cao, J., Tie, X., Xu, B., Zhao, Z., Zhu, C., Li, G., and Liu, S.: Measuring and modeling black carbon (BC) contamination in the SE Tibetan Plateau, J. Atmos. Chem., 67, 45–60, doi:10.1007/s10874-011-9202-5, 2010.
Cong, Z., Kang, S., Kawamura, K., Liu, B., Wan, X., Wang, Z., Gao, S., and Fu, P.: Carbonaceous aerosols on the south edge of the Tibetan Plateau: concentrations, seasonality and sources, Atmos. Chem. Phys., 15, 1573–1584, doi:10.5194/acp-15-1573-2015, 2015.
Gobbi, G. P., Angelini, F., Bonasoni, P., Verza, G. P., Marinoni, A., and Barnaba, F.: Sunphotometry of the 2006–2007 aerosol optical/radiative properties at the Himalayan Nepal Climate Observatory-Pyramid (5079 m a.s.l.), Atmos. Chem. Phys., 10, 11209–11221, doi:10.5194/acp-10-11209-2010, 2010.
Huang, J., Minnis, P., Yi, Y., Tang, Q., Wang, X., Hu, Y., Liu, Z., Ayers, K., Trepte, C., and Winker, D.: Summer dust aerosols detected from CALIPSO over the Tibetan Plateau, Geophys. Res. Lett., 34, L18805, doi:10.1029/2007gl029938, 2007.
Kahn, R. A.: Multiangle Imaging Spectroradiometer (MISR) global aerosol optical depth validation based on 2 years of coincident Aerosol Robotic Network (AERONET) observations, J. Geophys. Res., 110, D10S04, doi:10.1029/2004jd004706, 2005.
Kahn, R. A., Gaitley, B. J., Garay, M. J., Diner, D. J., Eck, T. F., Smirnov, A., and Holben, B. N.: Multiangle Imaging SpectroRadiometer global aerosol product assessment by comparison with the Aerosol Robotic Network, J. Geophys. Res.-Atmos., 115, D23209, doi:10.1029/2010jd014601, 2010.
Kaufman, Y. J., Tanre, D., and Boucher, O.: A satellite view of aerosols in the climate system, Nature, 419, 215–223, doi:10.1038/nature01091, 2002.
King, M. D., Kaufman, Y. J., Tanré, D., and Nakajima, T.: Remote sensing of tropospheric aerosols from space: past, present, and future, B. Am. Meteorol. Soc., 80, 2229–2259 1999.
Kuhlmann, J. and Quaas, J.: How can aerosols affect the Asian summer monsoon? Assessment during three consecutive pre-monsoon seasons from CALIPSO satellite data, Atmos. Chem. Phys., 10, 4673–4688, doi:10.5194/acp-10-4673-2010, 2010.
Li, Z., Li, C., Chen, H., Tsay, S. C., Holben, B., Huang, J., Li, B., Maring, H., Qian, Y., Shi, G., Xia, X., Yin, Y., Zheng, Y., and Zhuang, G.: East Asian Studies of Tropospheric Aerosols and

their Impact on Regional Climate (EAST-AIRC): an overview, J. Geophys. Res.-Atmos., 116, D00K34, doi:10.1029/2010jd015257, 2011.
Lin, C., Yang, K., Qin, J., and Fu, R.: Observed coherent trends of surface and upper-air wind speed over China since 1960, J. Climate, 26, 2891–2903, doi:10.1175/JCLI-D-12-00093.1, 2012.
Liu, D., Wang, Z., Liu, Z., Winker, D., and Trepte, C.: A height resolved global view of dust aerosols from the first year CALIPSO lidar measurements, J. Geophys. Res.-Atmos., 113, D16214, doi:10.1029/2007JD009776, 2008.
Liu, Z., Liu, D., Huang, J., Vaughan, M., Uno, I., Sugimoto, N., Kittaka, C., Trepte, C., Wang, Z., Hostetler, C., and Winker, D.: Airborne dust distributions over the Tibetan Plateau and surrounding areas derived from the first year of CALIPSO lidar observations, Atmos. Chem. Phys., 8, 5045–5060, doi:10.5194/acp-8-5045-2008, 2008.
Ma, J., Chen, Y., Wang, W., Yan, P., Liu, H., Yang, S., Hu, Z., and Lelieveld, J.: Strong air pollution causes widespread haze-clouds over China, J. Geophys. Res.-Atmos., 115, D18204, doi:10.1029/2009JD013065, 2010.
Ma, Y., Zhong, L., Wang, B., Ma, W., Chen, X., and Li, M.: Determination of land surface heat fluxes over heterogeneous landscape of the Tibetan Plateau by using the MODIS and in situ data, Atmos. Chem. Phys., 11, 10461–10469, doi:10.5194/acp-11-10461-2011, 2011.
Ma, Y., Han, C., Zhong, L., Wang, B., Zhu, Z., Wang, Y., Zhang, L., Meng, C., Xu, C., and Amatya, P.: Using MODIS and AVHRR data to determine regional surface heating field and heat flux distributions over the heterogeneous landscape of the Tibetan Plateau, Theor. Appl. Climatol., 117, 643–652, doi:10.1007/s00704-013-1035-5, 2014a.
Ma, Y., Zhu, Z., Zhong, L., Wang, B., Han, C., Wang, Z., Wang, Y., Lu, L., Amatya, P. M., Ma, W., and Hu, Z.: Combining MODIS, AVHRR and in situ data for evapotranspiration estimation over heterogeneous landscape of the Tibetan Plateau, Atmos. Chem. Phys., 14, 1507–1515, doi:10.5194/acp-14-1507-2014, 2014b.
Martonchik, J. V., Diner, D. J., Kahn, R., Gaitley, B., and Holben, B. N.: Comparison of MISR and AERONET aerosol optical depths over desert sites, Geophys. Res. Lett., 31, L16102, doi:10.1029/2004gl019807, 2004.
Sheng, J., Wang, X., Gong, P., Joswiak, D. R., Tian, L., Yao, T., and Jones, K. C.: Monsoon-driven transport of organochlorine pesticides and polychlorinated biphenyls to the Tibetan Plateau: three year atmospheric monitoring study, Environ. Sci. Technol., 47, 3199–3208, doi:10.1021/es305201s, 2013.

ACPD
15, 15683–15710, 2015

Tian, L., Yao, T., MacClune, K., White, J. W. C., Schilla, A., Vaughn, B., Vachon, R., and Ichiyanagi, K.: Stable isotopic variations in west China: a consideration of moisture sources, J. Geophys. Res., 112, D10112, doi:10.1029/2006jd007718, 2007.
Vernier, J. P., Thomason, L. W., and Kar, J.: CALIPSO detection of an Asian tropopause aerosol layer, Geophys. Res. Lett., 38, L07804, doi:10.1029/2010gl046614, 2011.
Winker, D. M., Hunt, W. H., and McGill, M. J.: Initial performance assessment of CALIOP, Geophys. Res. Lett., 34, L19803, doi:10.1029/2007gl030135, 2007.
Winker, D. M., Pelon, J., Coakley, J. A., Ackerman, S. A., Charlson, R. J., Colarco, P. R., Flamant, P., Fu, Q., Hoff, R. M., Kittaka, C., Kubar, T. L., Le Treut, H., McCormick, M. P., Mégie, G., Poole, L., Powell, K., Trepte, C., Vaughan, M. A., and Wielicki, B. A.: The CALIPSO mission: a global 3d view of aerosols and clouds, B. Am. Meteorol. Soc., 91, 1211–1229, doi:10.1175/2010BAMS3009.1, 2010.
Winker, D. M., Tackett, J. L., Getzewich, B. J., Liu, Z., Vaughan, M. A., and Rogers, R. R.: The global 3-D distribution of tropospheric aerosols as characterized by CALIOP, Atmos. Chem. Phys., 13, 3345–3361, doi:10.5194/acp-13-3345-2013, 2013.
Witek, M. L., Garay, M. J., Diner, D. J., and Smirnov, A.: Aerosol optical depths over oceans: a view from MISR retrievals and collocated MAN and AERONET in situ observations, J. Geophys. Res.-Atmos., 118, 12620–12633, doi:10.1002/2013JD020393, 2013.
Wu, G., Liu, Y., Zhang, Q., Duan, A., Wang, T., Wan, R., Liu, X., Li, W., Wang, Z., and Liang, X.: The influence of mechanical and thermal forcing by the Tibetan Plateau on Asian climate, J. Hydrometeorol., 8, 770–789, doi:10.1175/JHM609.1, 2007.
Wu, G., Liu, Y., He, B., Bao, Q., Duan, A., and Jin, F.-F.: Thermal controls on the Asian Summer Monsoon, Sci. Rep., 2, 404, doi:10.1038/srep00404, 2012.
Wu, G., Zhang, C., Xu, B., Mao, R., Joswiak, D., Wang, N., and Yao, T.: Atmospheric dust from a shallow ice core from Tanggula: implications for drought in the central Tibetan Plateau over the past 155 years, Quaternary Sci. Rev., 59, 57–66, doi:10.1016/j.quascirev.2012.10.003, 2013.
Xia, X., Wang, P., Wang, Y., Li, Z., Xin, J., Liu, J., and Chen, H.: Aerosol optical depth over the Tibetan Plateau and its relation to aerosols over the Taklimakan Desert, Geophys. Res. Lett., 35, L16804, doi:10.1029/2008gl034981, 2008.
Xia, X. G., Zong, X. M., Cong, Z. Y., Chen, H. B., Kang, S. C., and Wang, P. C.: Baseline continental aerosol over the central Tibetan plateau and a case study of aerosol transport from South Asia, Atmos. Environ., 45, 7370–7378, 2011.

Xu, B., Cao, J., Hansen, J., Yao, T., Joswia, D. R., Wang, N., Wu, G., Wang, M., Zhao, H., and Yang, W.: Black soot and the survival of Tibetan glaciers, P. Natl. Acad. Sci. USA, 106, 22114–22118, 2009.

Xu, C., Ma, Y. M., Panday, A., Cong, Z. Y., Yang, K., Zhu, Z. K., Wang, J. M., Amatya, P. M., and Zhao, L.: Similarities and differences of aerosol optical properties between southern and northern sides of the Himalayas, Atmos. Chem. Phys., 14, 3133–3149, doi:10.5194/acp-14-3133-2014, 2014.

Yao, T., Thompson, L., Yang, W., Yu, W., Gao, Y., Guo, X., Yang, X., Duan, K., Zhao, H., and Xu, B.: Different glacier status with atmospheric circulations in Tibetan Plateau and surroundings, Nature Clim. Change, 2, 663–667, 2012.

Yao, T., Masson-Delmotte, V., Gao, J., Yu, W., Yang, X., Risi, C., Sturm, C., Werner, M., Zhao, H., He, Y., Ren, W., Tian, L., Shi, C., and Hou, S.: A review of climatic controls on δ^{18}O in precipitation over the Tibetan Plateau: observations and simulations, Rev. Geophys., 51, 525–548, doi:10.1002/rog.20023, 2013.

ACPD
15, 15683–15710, 2015

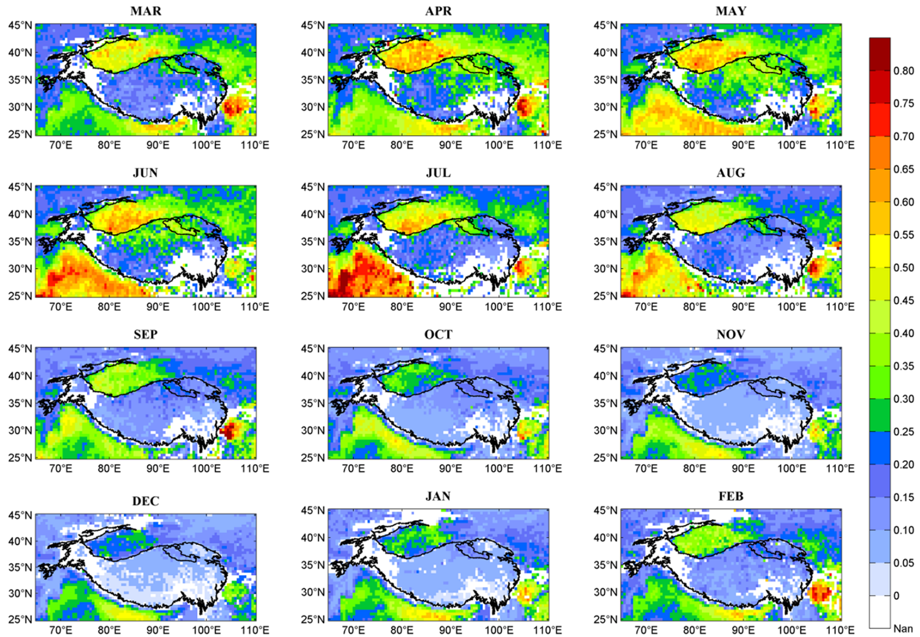

Figure 1. Monthly variations of AOD over the Tibetan Plateau. White shading indicates insufficient available data.

ACPD
15, 15683–15710, 2015

Regional distribution characteristics of aerosol optical depth

C. Xu et al.

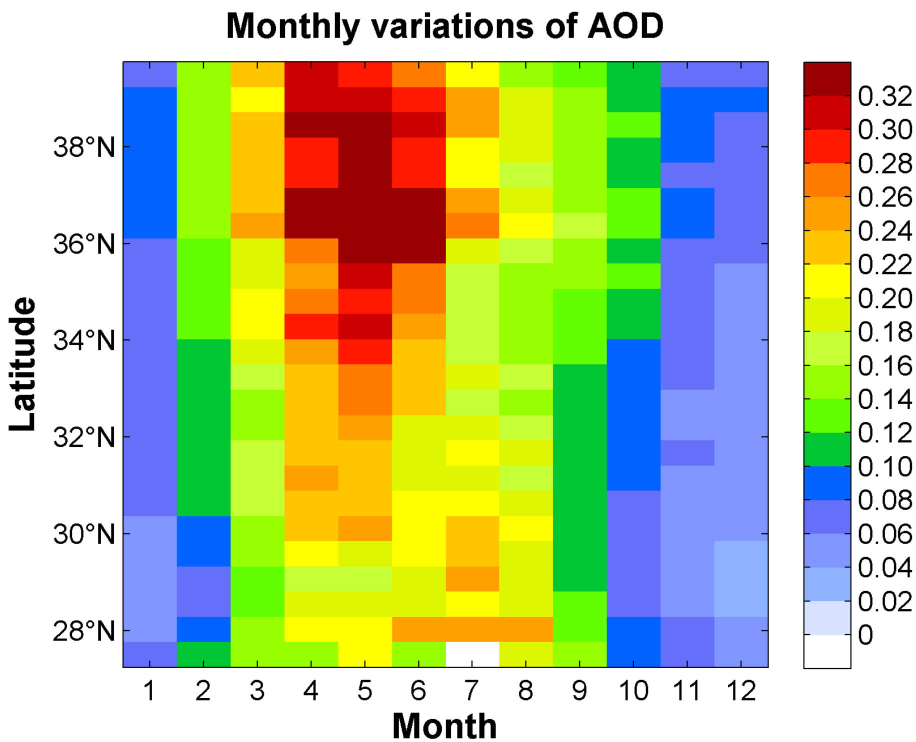

Figure 2. Zonal average of AOD over the Tibetan Plateau in each month. White shading indicates insufficient available data.

ACPD
15, 15683–15710, 2015

Regional distribution characteristics of aerosol optical depth

C. Xu et al.

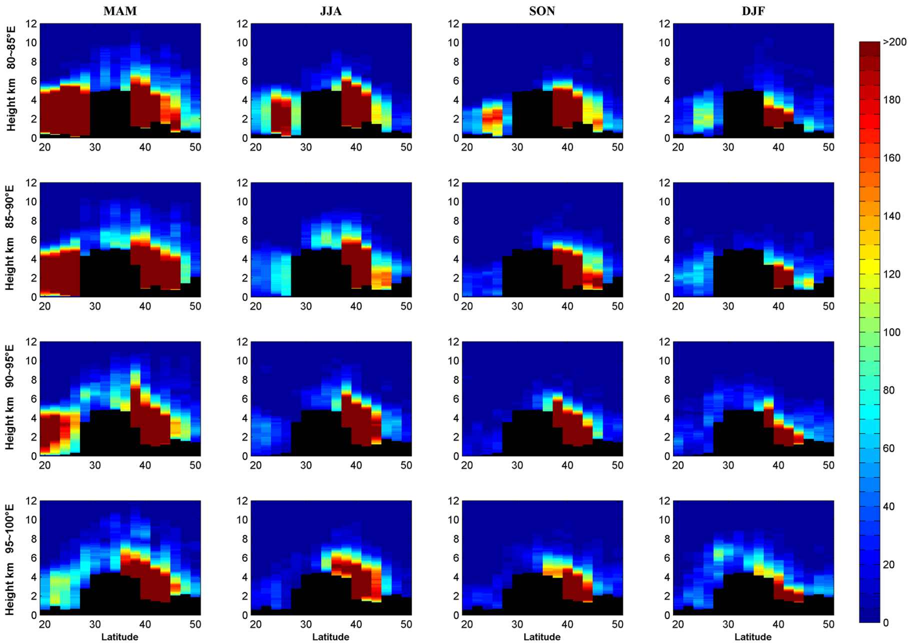

Figure 3. The detected accumulated dust samples for four seasons over the Tibetan Plateau and surrounding areas for four longitudinal transects (80–85, 85–90, 90–95 and 95–100° E). Black areas represent mountain profiles along the transects. MAM denotes March to May, JJA denotes June to August, SON denotes September to November and DJF denotes December to February in the next year (the following season divisions are the same).

ACPD
15, 15683–15710, 2015

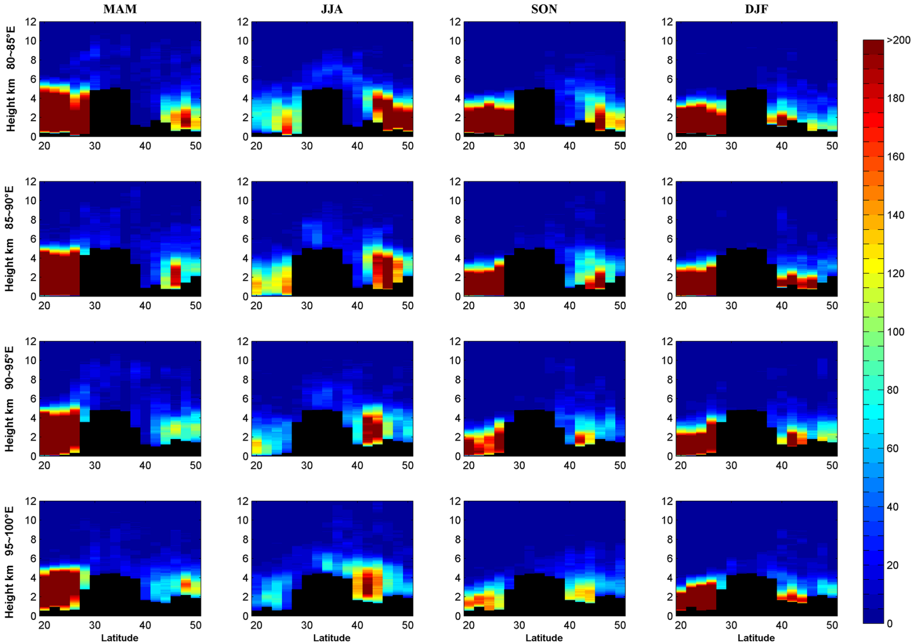

Figure 4. The detected accumulated polluted dust samples for four seasons over the Tibetan Plateau and surrounding areas for four longitudinal transects (80–85, 85–90, 90–95 and 95–100° E). Black areas represent mountain profiles along the transects.

ACPD
15, 15683–15710, 2015

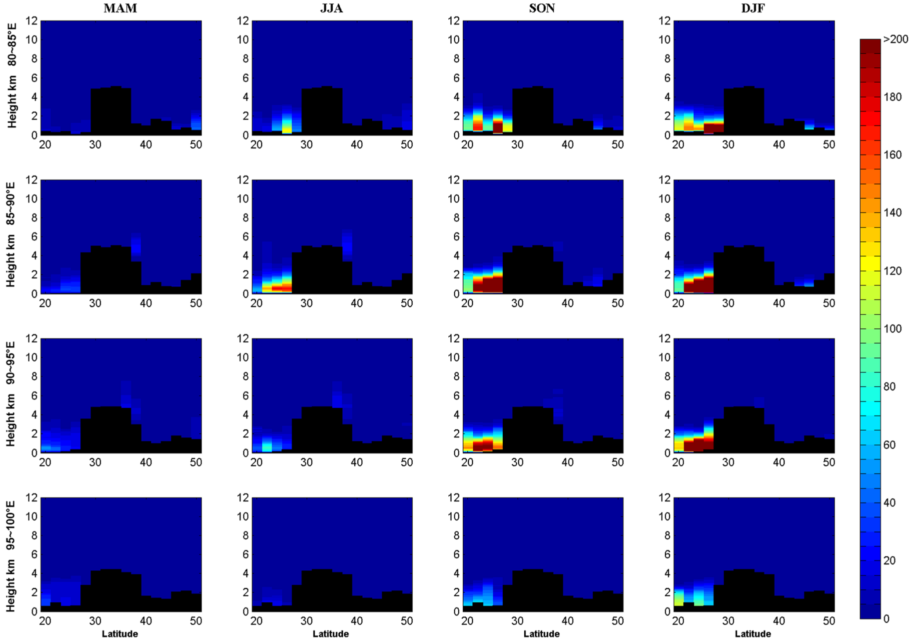

Figure 5. The detected accumulated polluted continental samples for four seasons over the Tibetan Plateau and surrounding areas for four longitudinal transects (80–85, 85–90, 90–95 and 95–100° E). Black areas represent mountain profiles along the transects.

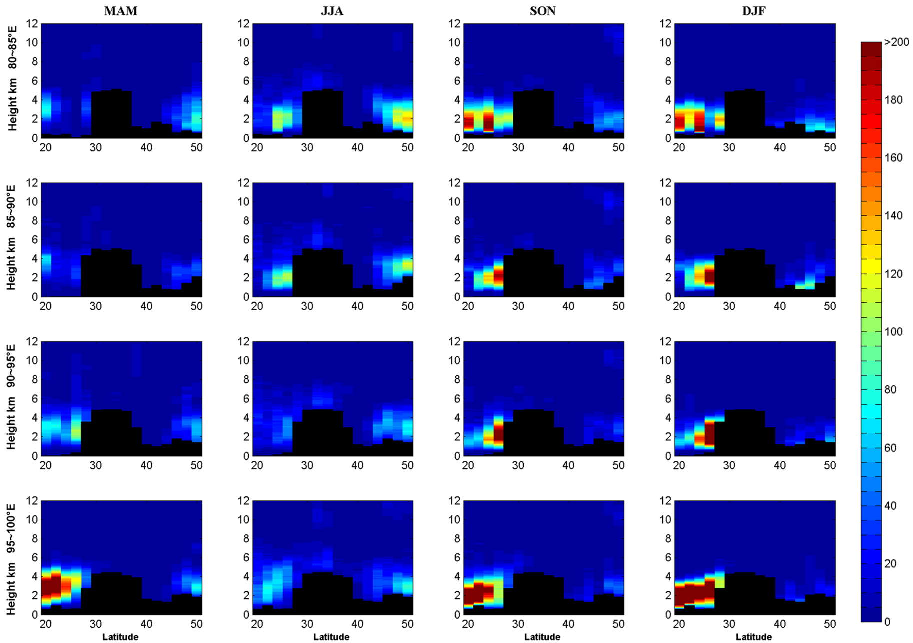

Figure 6. The detected accumulated smoke samples for four seasons over the Tibetan Plateau and surrounding areas for four longitudinal transects (80–85, 85–90, 90–95 and 95–100° E). Black areas represent mountain profiles along the transects.

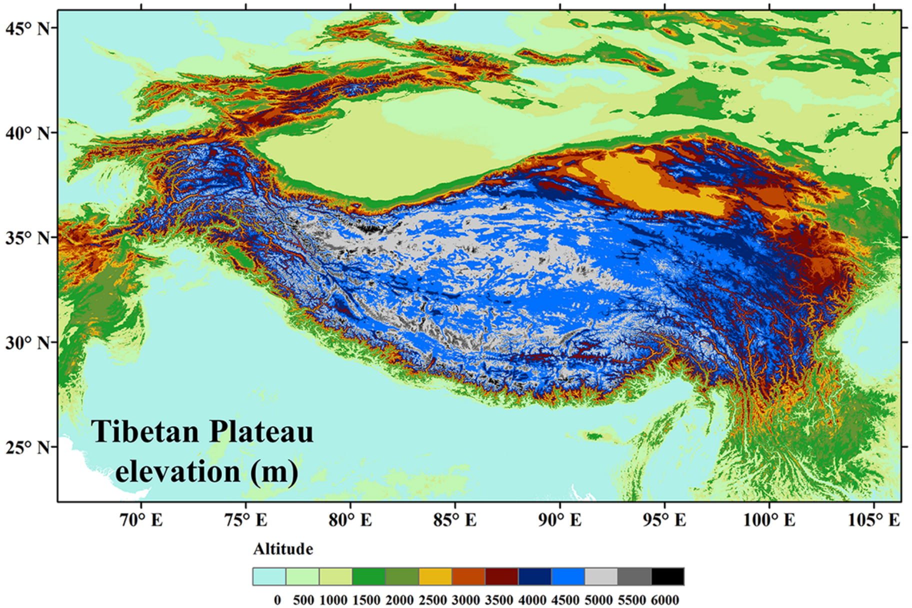

Figure 7. The topography (in m) of the Tibetan Plateau.

ACPD
15, 15683–15710, 2015

Regional distribution characteristics of aerosol optical depth

C. Xu et al.

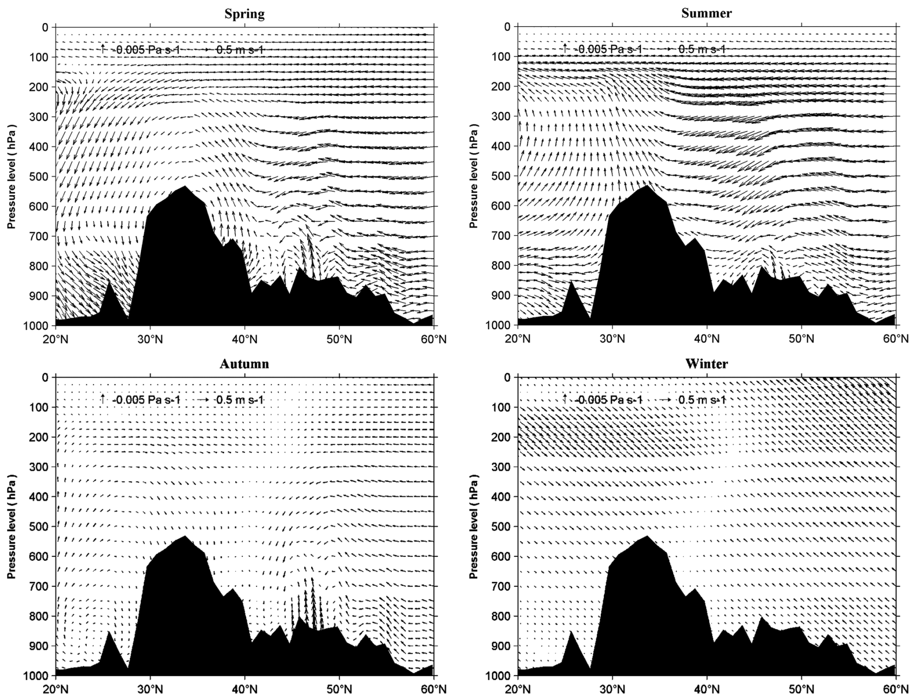

Figure 8. The meridional circulation at 95° E in the four seasons. The black shading shows the altitudes of the Tibetan Plateau at 95° E.

ACPD
15, 15683–15710, 2015

Regional distribution characteristics of aerosol optical depth

C. Xu et al.